Published in final edited form as:
Acad Radiol. 2015 January ; 22(1): 33–49. doi:10.1016/j.acra.2014.08.011.

Clinical Utility of Quantitative Imaging

Andrew B Rosenkrantz, MD MPA
Department of Radiology NYU Langone Medical Center 550 First Avenjue New York, NY 10016

Mishal Mendiratta-Lala, MD
Henry Ford Hospital Abdominal and Cross-sectional Interventional Radiology 2799 West Grand Boulevard Detroit, MI 48202

Brian J. Bartholmai, M.D.
Division of Radiology Informatics Mayo Clinic in Rochester, MN 200 First Street SW Rochester, MN 55905

Dhakshinamoorthy Ganeshan, MD
Department of Abdominal Imaging University of Texas MD Anderson Cancer Center 1515 Holcombe Blvd #207 Houston, Texas 77030

Richard G. Abramson, MD
Department of Radiology and Radiological Sciences Vanderbilt University School of Medicine 1161 21st Ave. S, CCC-1121 MCN Nashville, TN 37232-2675

Kirsteen R. Burton, MBA, MSc, MD
Dept. of Medical Imaging and Institute of Health Policy, Management and Evaluation University of Toronto 263 McCaul Street, 4th Floor Toronto, ON M5T1W7

John-Paul J. Yu, MD, PhD
Department of Radiology and Biomedical Imaging University of California, San Francisco 505 Parnassus Ave., M-391 Box 0628 San Francisco, CA 94143-0628

Ernest M. Scalzetti, MD
Department of Radiology SUNY Upstate Medical University 750 E. Adams St. Syracuse NY 13210

Thomas E. Yankeelov, PhD
Institute of Imaging Science Vanderbilt University 1161 21st Ave South, AA 1105 MCN Nashville, TN 37232-2310

Rathan M. Subramaniam, MD, PhD, MPH
Russell H Morgan Department of Radiology and Radiological Sciences, Johns Hopkins School of Medicine Department of Health Policy and Management, Johns Hopkins Bloomberg School of

Corresponding Author: Andrew B Rosenkrantz, MD MPA Department of Radiology NYU Langone Medical Center 550 First Avenjue New York, NY 10016 Phone: (212)263-0232 Fax: (212)263-6634 Andrew.Rosenkrantz@nyumc.org.

Public Health Johns Hopkins University, Baltimore, MD 601 N. Caroline Street Baltimore, MD 21287

Leon Lenchik, MD
Department of Radiology Wake Forest School of Medicine Medical Center Boulevard Winston-Salem, NC 27157

Abstract

Quantitative imaging (QI) is increasingly applied in modern radiology practice, assisting in the clinical assessment of many patients and providing a source of biomarkers for a spectrum of diseases. QI is commonly used to inform patient diagnosis or prognosis, determine the choice of therapy, or monitor therapy response. Because most radiologists will likely implement some QI tools to meet the patient care needs of their referring clinicians, it is important for all radiologists to become familiar with the strengths and limitations of QI. The Association of University Radiologists Radiology Research Alliance Quantitative Imaging Task Force has explored the clinical application of QI and summarizes its work in this review. We provide an overview of the clinical use of QI by discussing QI tools that are currently employed in clinical practice, clinical applications of these tools, approaches to reporting of QI, and challenges to implementing QI. It is hoped that these insights will help radiologists recognize the tangible benefits of QI to their patients, their referring clinicians, and their own radiology practice.

Keywords

radiology; radiologist; quantitative imaging; biomarker

INTRODUCTION

Quantitative imaging (QI) is becoming an increasingly common tool in modern radiology practice, advancing from research trials to clinical reading rooms. Today, methods that quantify imaging features assist in the clinical assessment of many patients, serving as biomarkers for disease states as diverse as brain ischemia, interstitial lung disease, and colorectal cancer. Because the potential impact of QI on patient care and on clinical outcomes is so great, the Radiological Society of North America has committed considerable resources to standardizing QI, most recently with the Quantitative Imaging Biomarkers Alliance (QIBA). The Association of University Radiologists' leadership, QIBA participants, and many others in the radiology community view QI as important to the future of radiology. Because it is anticipated that most practicing radiologists will eventually implement some QI tools to meet the specific patient care needs of their referring clinicians, it is important for radiologists of all subspecialties and practice types to become familiar with the various strengths and limitations of QI.

What is Quantitative Imaging? According to QIBA(1):

> “Quantitative imaging is the extraction of quantifiable features from medical images for the assessment of normal or the severity, degree of change, or status of a disease, injury, or chronic condition relative to normal. Quantitative imaging

> includes the development, standardization, and optimization of anatomical, functional, and molecular imaging acquisition protocols, data analyses, display methods, and reporting structures. These features permit the validation of accurately and precisely obtained image-derived metrics with anatomically and physiologically relevant parameters, including treatment response and outcome, and the use of such metrics in research and patient care."

While this definition is comprehensive, several practical aspects of QI must be highlighted: accuracy, precision, and clinical validity. When performing measurements, we must be certain that what we are measuring has a clinical correlate, a reference standard against which our measurement has been derived. In this regard, the accuracy of a measurement describes how close the measurement is to a correct answer and thus indicates whether our QI measurement fundamentally "works." Precision is also important, particularly given the role of QI in performing serial evaluation over time. A useful QI metric should provide the same value when measured in the same way multiple times. Precision (repeatability and reproducibility) allows us to discriminate measurement error from biologic change. Finally, QI tools that demonstrate good accuracy and reliability must ultimately have clinical validity; the results must be relevant to our practice, impacting patient care and improving outcomes.

QI has the greatest impact on patient care when the results help to: (1) inform the diagnosis or prognosis of a particular disease; (2) determine the choice of a particular therapy; or (3) monitor the course of therapy. To make the diagnosis using QI, a general consensus of normal versus abnormal QI values must be established. Similarly, monitoring the response to therapy with QI requires consensus on the amount of change that is considered both statistically and clinically significant. This paper will present an overview of the clinical use of QI by presenting QI tools that are currently used in clinical practice, clinical applications of these tools, approaches to reporting that add value to clinical care, and challenges to implementing QI in a clinical radiology practice.

TOOLS FOR PERFORMING QUANTITATIVE IMAGING

Image Acquisition

QI currently has important clinical applications in ultrasound, computerized tomography (CT), magnetic resonance imaging (MRI), and nuclear medicine, including position emission tomography (PET), although theoretically can be applied to any digital imaging modality. QI is enhanced by volumetric data sets, which facilitate assessments of morphological, parametric, functional, and other quantitative features.

Ultrasound—Gray-scale ultrasound images are commonly used to obtain size and distance measures, providing the basis for diagnosis in much of obstetric and cardiac imaging. Doppler ultrasound, in which altered frequency of the reflected sound waves provides measurements of flow velocity, has been used for quantitative characterization of vascular disease for decades (2). Flow velocities are routinely used in the diagnosis of vascular stenoses of the carotid and renal arteries, transplant vasculature, and vascular shunts (2, 3) (Figure 1). More sophisticated Doppler measures such as the intrarenal acceleration time and

resistive index are used in diagnosing renal artery stenosis (4). Technical optimization of Doppler including angle correction, gain, and gate position, is essential to avoid measurement errors (5).

CT—The standardization of CT pixel values with the Hounsfield Unit (HU) scale allows for characterization of tissue density, a common QI application (6). HU measures allow lesion characterization using region-of-interest (ROI) based measurement of average density or voxel-counting based on a threshold value (7). For instance, improved characterization of renal lesions is achieved using ROI measurements rather than subjective visual assessment (8).

Recently, the advent of dual-energy CT (DECT) scanners has bolstered the clinical role of QI, as the differential absorption of x-rays by tissues of differing chemical composition at different energies allows for improved characterization of tissues (9) (Figure 2). For instance, DECT has greater accuracy than standard single-energy CT in determining the composition of renal calculi (10). This distinction helps determine whether a patient is treated medically or with an invasive procedure such as extracorporeal shockwave lithotripsy.

MRI—Given its ability to interrogate various properties of tissues using specific pulse sequences and various vascular and tissue-specific contrast agents, MRI is ideally suited for QI (6). MR signal intensity (SI) units lack inherent meaning, being influenced by sequence parameters, as well as hardware and software selection. However, some advanced MRI sequences and post-processing techniques allow for the computation of parametric maps in which the pixel values are used for diagnosis. For example, imaging the liver using varying echo times (TEs) allows for computation of the tissue T2* relaxation time, used as a marker of the presence and severity of hepatic deposition (11) (Figure 3). Diffusion-weighted (DW) MRI using a rapid echo-planar sequence with motion-probing gradients of varying strength, as reflected by the b-value, allows for computation of the apparent diffusion coefficient (ADC) of tissue (12). Lower ADC values occur in more cellular tissues and serve as markers for the presence and aggressiveness of tumors, such as prostate cancer (12, 13). Diffusion-tensor imaging (DTI) is an extension of DW-imaging that provides quantification of white matter tracts to guide surgery for brain tumors, allowing for better definition of surrounding neural pathways and improving functional outcomes (14). MRI spectroscopy provides information regarding the presence and concentration of chemicals in an ROI, such as brain metabolites that show characteristic alterations in conditions including Alzheimer's disease, infection, tumor, and radiation therapy (15). In addition, rapid MRI techniques, including real-time “segmented” sequences and velocity-encoded phase-contrast imaging, are used in cardiac imaging to calculate stroke volume and cardiac output (16).

Dynamic Contrast-Enhanced Imaging—Dynamic contrast-enhanced CT or MRI is often used to improve tissue characterization. Rapid contrast administration and imaging the same region at multiple time-points allows a comparison of pixel values between pre- and post-contrast images and assessment of the rate and pattern of enhancement or washout over time. For example, after contrast administration, an increase in pixel values for a renal lesion of at least 20 HU on CT or of at least 15% on MRI indicates a solid lesion (17, 18).

Obtaining a larger number of post-contrast time-points provides a more precise assessment of the temporal kinetics of contrast passage through a tissue. Although a lack of ionizing radiation with MRI generally allows acquisition of more time-points than with CT, the non-linear relationship between tissue gadolinium concentration and MRI signal intensity complicates the computation of kinetic parameters (19). Various approaches to post-processing and quantification of multi-phase post-contrast imaging are used. For example, time-activity curves are routinely applied for tumor detection in breast MRI (20), while multi-compartment pharmacokinetic models provide quantitative metrics for evaluation of gliomas and other tumors (21).

General Nuclear Medicine and PET—Many general nuclear medicine examinations include dynamic acquisition and count-based regional detection of radiopharmaceutical to quantify the physiology of an organ. For example, left ventricular ejection fraction, gastric emptying, and individual renal function may be computed using technitium99m labeled red blood cells, sulfur colloid, and MAG3, respectively. PET is a powerful tool for evaluating tissue metabolism, most commonly using the glucose analog ^{18}F-fluoro-deoxyglucose (FDG) (22). The standardized uptake value (SUV) represents the concentration of radioactivity within a tissue, normalized by dividing it by the ratio between the decay-corrected injected radioactivity and the patient's body weight, lean body mass, or surface area (23, 24). SUVs are used to determine the likelihood of malignancy of lesions as well as to predict tumor aggressiveness and treatment response (25, 26). For example, in gastrointestinal stromal tumors, a reduction in SUV is a better measure of treatment response than a decrease in lesion size (27). New PET-based parameters such as metabolic tumor volume (MTV), total lesion glycolysis (TLG), and heterogeneity index, are also being applied in clinical decision making; for instance, these metrics have been used to distinguish human papillomavirus (HPV)-positive and HPV-negative primary oropharyngeal squamous cell carcinoma (28).

Quality Assurance

In an effort to standardize acquisition and improve reproducibility of QI metrics, expert panels have provided recommendations regarding acquisition techniques (6). Standardized protocols and attention to both hardware and software are important (6, 29, 30). With MRI, sequence parameters as well as coil selection and positioning have a major impact on quantitative measurements. In nuclear medicine, many examinations require standardized conditions and patient-specific adjustment, including monitoring of serum glucose and ensuring a period of fasting prior to the study, in addition to daily equipment calibration using a phantom. With CT, the kernel, slice thickness, and artifacts alter regional and overall HU. The ACR accreditation process and most vendor recommendations require scanners to undergo daily calibration and regular quality assurance with a phantom to validate HU accuracy. Image quality must be balanced with radiation dose reduction and monitoring (31). Consistent calibration and acquisition protocols do not assure that results from different devices will be equivalent. Nonetheless, most QI tools are designed to be valid for specific modalities within a defined range of acquisition parameters.

The importance of standardized acquisition parameters is evident when using CT to monitor serial changes in tumor volume. Differences in volume-averaging effects, segmentation, and density characteristics may impact volume calculations. Serial CT acquisitions should use similar contrast agent dose and injection rate, consistent positioning of the patient, comparable breath-holding instructions, the same scanner platform, and equivalent or comparable acquisition and reconstruction parameters (32). When adhering to these recommendations, data suggest that a change of over 30% in tumor volume provides at least 95% probability that there is a true change (32). Similarly, when using DCE-MRI to monitor and predict treatment response of solid tumors at least 2 cm in size, standardized acquisition parameters allow for a reliable quantitative assessment of the K^{trans} of the tumor. Specifically, a change of approximately 40% in K^{trans} is considered to represent a significant change (33). Repeatability of QI metrics is well established for PET and is generally in the range of 15–20% when following standardized protocols (34, 35).

Lesion Measurement

Although the size of structures is often reported using diameters, for many clinical applications, including evaluation of tumors, size is better represented in terms of volumes (36). This approach provides a more accurate representation of the size of a lesion with an irregular shape or contour and in which a change in diameter may not reflect a change in volume (29, 37). There are many approaches for determining lesion volume. One approach is to estimate the volume using the prorate ellipsoid formula based on a single measurement in all three dimensions (38). Although straightforward, this formula may be less accurate if the lesion's shape deviates substantially from a sphere. Planimetry is a more reliable, yet more time-consuming, method for measuring volume in which the edge of the structure is traced on all image slices and cross-sectional areas are summed and multiplied by the slice thickness (39) (40). Finally, specialized software may be used to recognize the edges of structures, for example using threshold-based, connected components, or region-growing algorithms, to segment an organ or lesion and thereby automate determination of volumes (41), for instance in evaluating tumor metabolic volume using PET (42).

In addition to measuring the size of a structure, QI often includes measurement of the value of the numerous voxels comprising a lesion. The voxels within a segmented area comprise a ROI, and an overall value representing the distribution or features of voxel values within the ROI can be determined (30). The mean value of the ROI (which may represent HU, SUV, ADC, flow velocities or many other imaging-based measures) or distribution of voxel values within the ROI including the minimum, median, and maximal values may all have distinct clinical applications. For example, both the minimum ADC (43) value and the maximum SUV (44) may help characterize brain tumors. The pixel values within the ROI may also be weighted to produce a volume- and character-based score, such as done for coronary calcium scoring (45).

For some clinical applications, a probabilistic measure that reflects a combination of numerous imaging parameters is more relevant than a single parameter (46) and is especially useful for standardizing the reporting of findings that are based on complex multi-parametric evaluation. For example, the Breast Imaging Reporting and Data Systems (BI-RADS)

provides a standardized grading scheme that incorporates various mammographic findings, including the shape, size, margins, density, and others to distinguish benign and malignant lesions (47).

CLINICAL APPLICATIONS OF QUANTITATIVE IMAGING

In this section, we discuss select clinical applications of QI based on different organ systems. Representative examples are also presented in Table 1.

Abdominal Imaging, including Oncologic Imaging

One of the most commonly used QI techniques in abdominal imaging is image-derived tumor measurements to monitor disease progression and therapy response (48) (Figure 4). QI results predict drug efficacy and alter timing or type of treatment (49, 50). In some settings, there is a need to summarize properties of multiple lesions across multiple organs over time to monitor overall tumor burden. The Response Evaluation Criteria in Solid Tumors (RECIST) is one commonly used approach for monitoring response of metastatic lesions to drug therapies, taking into account the number and size of lesions (51). RECIST criteria require baseline documentation of target and non-target lesions, providing a sum of diameters of all target lesions. On follow-up imaging, the disease burden is categorized as a complete response, a partial response, progressive disease, or stable disease, based mainly on the sum of diameters of target lesions (51). Despite the enthusiasm for RECIST among oncologists, its potential for accurately determining tumor response is limited by its reliance on lesion diameters. A more complete assessment of tumor response may require combining changes in lesion size with other quantitative and molecular imaging markers (Figure 5, 6). The recently proposed Choi criteria take into account both the size and CT attenuation of lesions and provide a better assessment of treatment response of metastatic gastrointestinal stromal tumors (52) and renal cell carcinoma (53) than RECIST criteria. Various other response criteria, such as European Organisation for Research and Treatment of Cancer (EORTC), PET Response Criteria in Solid Tumors (PERCIST), and Deauville criteria, have been developed for PET (54, 55). For example, Deauville PET criteria are incorporated into the National Comprehensive Cancer Network (NCCN) guidelines for management of Hodgkin's lymphoma (55).

QI is commonly used in evaluating incidental adrenal nodules, helping differentiate benign from potentially malignant adrenal nodules that require further work-up. On a non-contrast CT, an adrenal nodule HU measurement of <10 has nearly 100% specificity for a lipid rich benign adrenal adenoma (56) (Figure 7). However, if the HU measurement is greater, further characterization may be warranted, usually with in-and-opposed-phase MRI or adrenal wash-out protocol CT (57). The CT adrenal washout protocol includes acquisition of multiple phases to allow calculation of either the absolute or relative washout ratios (58) (Figure 8). For adrenal lesions that remain indeterminate, using a combination of CT and PET criteria has been shown to achieve 99% accuracy in characterization (59).

QI is also used in oncologic imaging for determining response to therapy by evaluating lesion attenuation or contrast enhancement before and after treatment. With therapy, some tumors do not decrease in size but instead show a decrease in vascularity or density that

indicates tumor necrosis (Figure 9). For example, certain types of gastrointestinal stromal tumors show a decrease in density on CT but do not generally regress in volume following therapy (60). Similarly, the main goal of locoregional therapy for hepatocellular carcinoma (HCC) is necrosis of the tumor as opposed to tumor shrinkage (61), which is assessed by changes in enhancement characteristics on dynamic post-contrast CT and MRI (62). Finally, histogram assessment of a whole-lesion or whole-disease burden ROI avoids the sampling error of a partial-lesion ROI and better reflects lesion texture and heterogeneity. Metrics derived from this approach, such as skewness and kurtosis, have been applied for monitoring treatment response to various malignancies, including metastatic ovarian and primary peritoneal cancer(63).

Neuroimaging

QI has an essential role in improving clinical management and outcome of acute ischemic stroke (64). Quantitative analysis of blood flow (i.e., perfusion) to ischemic tissue provides essential information for treatment planning. Perfusion imaging is performed using single-photon emission computed tomography (SPECT), CT, and MRI (particularly DWI). Perfusion imaging helps evaluate tissue viability and reversibility of ischemia, and can predict the outcome of treatment (65) (Figure 10). While SPECT can only measure cerebral blood flow (CBF), CT perfusion has the advantage of also measuring cerebral blood volume (CBV) and mean transit time (MTT). CBV and CBF can be used together to identify acute ischemic stroke patients with large areas of ischemic penumbra who may benefit from thrombolytic therapy (65, 66). Furthermore, quantitative criteria derived from CT or MR perfusion are being incorporated into guidelines for determining stroke patients eligible for an extended window for thrombolysis(67). In acute stroke, advantages of CT perfusion over MRI with DWI include lower cost, higher availability, ease of patient monitoring, increased imaging speed, and the ability to acquire dynamic and angiographic images simultaneously (64, 68–70).

QI is also used in the evaluation of brain tumors, particularly in differentiating low from high grade gliomas. While standard CT and MRI provide anatomical characterization of gliomas, tumor grade, treatment effects, and recurrence are not reliably distinguished. This is achieved in PET with the use of FDG for glucose metabolism and C-11 methionine (MET) for amino acid transportation (71). Quantitative analysis with PET and MR spectroscopy are used for grading of tumors and estimating prognosis, differentiating tumor recurrence from post-radiation necrosis, evaluating treatment response, and defining a target volume for radiation therapy. SUV values from PET help distinguish high-grade and low-grade gliomas (72, 73). Patients with higher grade gliomas show ratios of tumor to contralateral normal brain glucose utilization at 1.4:1 or greater, which is associated with decreased median survival compared with lower metabolite ratios (72). On CT, higher grade gliomas also exhibit greater CBV and other perfusion metrics (74).

Functional MRI (fMRI) based on blood-oxygen level dependent (BOLD) imaging, provides maps correlating specific regions in the brain with language, motor function, and other tasks. In patients with brain tumors undergoing surgical evaluation, the proximity of such regions to the tumor impacts determination of the surgical risk, selection between surgery and other

treatments, and, in those patients who ultimately do undergo resection, planning of the surgical approach(75, 76).

Cardiac Imaging

The multi-gated acquisition (MUGA) scan is a commonly used QI tool in nuclear medicine that evaluates cardiac ventricular function. MUGA scans provide a cine image of the beating heart, from which mathematical models determine the left ventricular ejection fraction (LVEF) (77), used to diagnose congestive heart failure, to evaluate patients on cardiotoxic chemotherapeutic agents, and to assess patients with valvular disease or prior cardiac angioplasty bypass, or transplant. A normal LVEF is greater than 50, without abnormal wall motion (78). In patients receiving adriamycin, a subtle reduction in LVEF from the pre-treatment value can indicate subclinical cardiac toxicity and lead to discontinuing the drug in order to avoid cardiotoxicity (79).

Gated CT and MRI provide a comprehensive anatomic and physiologic cardiac assessment, including not only cardiac volumes and wall thickness, but also cardiac function, wall stress, and myocardial perfusion (80). Such QI results are used in managing patients with congenital cardiac anomalies, myocardial infarction, and congestive heart failure. In addition, coronary artery calcium scoring using non-contrast CT is commonly used as a screening study for coronary artery disease in patients with cardiac risk factors (81). Finally, anatomic information regarding sizes and relationships of vessels obtained from CT or MR angiography, in combination with flow information from Doppler ultrasound and advanced MRI sequences for flow quantification, provide useful information in surgical planning for vascular procedures, such as endovascular aneurysm repair and transcatheter aortic valve replacement (82).

Musculoskeletal Imaging

MRI is widely used in the clinical management of osteoarthritis (83). MRI allows quantitative measurements of articular cartilage, subchondral bone, menisci, ligaments, and synovium (84–86). In particular, measurements of articular cartilage thickness, volume, and surface area, help predict disease progression and guide treatment selection (87).

QI is also used in bone marrow evaluation. Compared with conventional T1 and T2 weighted MRI, quantitative chemical shift MRI helps distinguish and measure fat and water content to permit a more quantitative assessment of bone marrow composition (88, 89). This more accurately assesses post-treatment changes in patients with bone marrow infiltrating disorders and guides selection of patients for bone marrow transplantation in leukemia (90).

Obstetric Imaging

Fetal ultrasound imaging is used to evaluate intrauterine growth abnormalities. Various measurements are obtained, including head circumference (HC), biparietal diameter (BPD), abdominal circumference (AC) and femur length (FL) (91, 92) (Figure 11). These values are entered into a biometric calculator, examples of which are available on-line (93) as well as on the ultrasound console, from which an estimated fetal weight (EFW) and growth percentages are determined. Evaluation of the EFW and percentages with respect to the

patient's prior ultrasound and last menstrual period allows for the determination of intrauterine growth restriction (IUGR). In patients with suspected IUGR, presence of both EFW and AC less than the tenth percentile is associated with poor peripartum outcome (94). Based on fetal ultrasound findings, some patients are placed in a special follow-up category, which may consist of weekly Doppler ultrasound and follow-up growth evaluation in order to determine the need for bed rest and early fetal delivery to prevent fetal complications.

REPORTING OF QUANTITATIVE IMAGING STUDIES

With traditional qualitative reporting, subjectivity, variable descriptive language, reliance on a combination of experience, expertise, and opinion, and limitations inherent to human visual perception, all result in high variability between radiologists (95–97). Quantitative reporting of disease processes may help overcome such limitations.

While radiologists already evaluate some quantitative metrics during image interpretation, it is important to incorporate these metrics into the report, as is common practice for SUV values in PET and BI-RADS in mammography. At present, reporting of quantitative measures is not consistent. For example, in Doppler ultrasound, velocities and secondary-derived metrics are usually obtained and viewed by the radiologist, but are often not included in the report. Likewise, with CT, the radiologist may not report a HU measurement used to arrive at the correct diagnosis. Such lack of reporting may lead to additional unnecessary testing. For instance, when describing a homogeneous hyperdense renal lesion on a non-contrast CT, a HU measurement of the lesion over 70 should be included in the report to substantiate a diagnosis of a hemorrhagic/proteinaceous renal cyst (98), rather than a renal neoplasm, thus avoiding further imaging.

Standard qualitative reports are readily available as text from the radiology information system (RIS) and electronic medical record (EMR). In comparison, current clinical QI reporting applications tend to be modality, anatomy, disease, or parameter specific (Figure 12–14). As such, they may comprise a stand-alone software package, an individual function within a suite of image post-processing tools, or software integrated into an imaging modality itself. Given the multitude of vendors, modalities, organ systems, and applications available for QI, the format of the output is variable. Unfortunately, the evaluation of the same data by different systems may yield different results, not only due to distinct algorithms and processing strategies, but also due to variations in the visualization scheme and techniques utilized to export the numerical results from the application. For example, different software applications for quantitative evaluation of a coronary calcium score may use different thresholds for detection or formulae for calculation of volume based on the density of the pixels, resulting in slightly different scores. Such differences in generating the output of different software may only be apparent within the viewer itself, and not apparent when viewing output that is exported in the form of a text report, numerical spreadsheet, Extensible Markup Language (XML) document, or screen capture.

Comparison of quantitative results between different software packages or evaluation of results over time can be difficult. How QI results are stored in the medical record and how those are either recalled or historical data is reprocessed for comparison purposes is a non-

trivial problem. Many image processing solutions maintain a proprietary database to assure that the original numerical data is stored for reference and temporal comparison purposes or provide for analysis of more than one dataset at a time (such as a pulmonary nodule volumetric analysis tool that might determine doubling time). How the numerical results are archived and distributed for clinical consumption external to the processing system is variable.

The Digital Imaging and Communications in Medicine (DICOM) standard accommodates both storage of numerical data within the schema of a `Structured Report' (DICOM SR) as well as storage of proprietary data within custom fields in the DICOM header information of an image. Compared to current approaches for visualization of numerical data (i.e., simple screen capture of text annotations, numerical tables, or colored region-of-interest overlays of anatomic image data by physiologic parametric data) this approach is promising. Unfortunately, many modern PACS, RIS, and EMR systems cannot store or display the content of a DICOM SR object. Similarly, the reporting tools available for radiologists are often not capable of automatically incorporating data from a DICOM SR, XML or other `standard' quantitative results. Thus, reporting of QI data in a manner that is fully integrated into clinical workflow remains a challenge.

CHALLENGES TO QUANTITATIVE IMAGING IN CLINICAL PRACTICE

Since QI often provides information that can be difficult to assess through qualitative visual interrogation, it is somewhat surprising that there is a significant resistance in adopting QI in routine clinical care (99). We review various obstacles that hinder wider acceptance of QI in clinical practice.

Radiologists

Although some aspects of QI may be automated or semi-automated, the additional processing of sophisticated dynamic, multimodality fusion, or parametric analysis techniques requires significantly more time, effort, and expertise from radiologists compared to qualitative interpretation (100). Radiologists doing QI spend considerable time validating automated or semi-automated results, often using specialized software, which requires education of technologists and implementation of a quality assurance plan, creating burden for the radiologist. With increasing emphasis on productivity, time spent performing QI may be considered financially unrewarding. There are also practical hurdles to incorporation of QI results presented in tabular or graphical forms into radiology reporting workflows. Additional technical limitations relate to storing QI results in existing radiology systems, retrieving historical results, utilizing QI applications on serial exams, and distributing QI results to the EMR in a way that clinicians can access.

There is also concern that QI methods may not be validated or may provide misleading results to clinicians. For example, automated detection marks generated by breast or lung nodule CAD tools, although generally helpful for interpretation, are often incorrect and prone to misinterpretation by someone lacking experience in the tool's sensitivity, specificity, and overall limitations (101). Some of the skepticism in QI arises from a lack of sound guidelines or evidence regarding validity of currently available QI methods. For

instance, the use of QI in monitoring response to molecularly targeted therapies in patients with advanced renal cell carcinoma is controversial. Although RECIST and revised RECIST criteria are widely used, RECIST criteria alone may result in significant underestimation of early treatment response (102, 103). This is especially true for molecular targeted therapies that decrease tumor vascularity, causing tumor necrosis, without significant change in tumor size. To address this issue, newer criteria such as CHOI criteria, modified Choi criteria, SACT criteria, and MASS criteria have been proposed (53, 104–106). The lack of clear guidelines leads to confusion among radiologists as to which QI method is most appropriate for a given disease process.

Given these factors, it is understandable that there is some antipathy among radiologists towards QI (107). To overcome some of the challenges, it is essential to increase awareness of the impact of QI on patient management. As molecular medicine is making it clear that many disease processes have individual molecular signatures, appropriate patient management will increasingly depend on radiologists' ability to provide information not just on morphology, but also on biochemical and physiological changes. In order to make these tests clinically meaningful and ultimately benefit patients, radiological interpretations will need to incorporate QI.

Patients

Patients may be reluctant to undergo QI examinations because of additional time required for some functional tests (100) or, in some circumstances, because of additional expense associated with the post-processing needed to produce QI results. Similarly, multi-phase or dual-energy CT examinations may require additional radiation exposure that may be less desirable to the patient. The value of QI and advanced image analysis may be difficult to explain to a patient given the availability of multiple tests that provide similar, albeit distinctly different, results. For example, a pulmonary function test may be used to assess global pulmonary function in COPD, cystic fibrosis or interstitial lung disease. However, QI metrics provide pulmonary parenchymal, vascular, and airway analysis that is more disease-specific and helps direct specific therapy. With emphysema, semi-quantitative visual or threshold-based density assessment of the lungs using QI can help determine whether medical therapy, lung volume reduction surgery, or transplantation is likely to be most efficacious (108, 109). Nonetheless, convincing a patient that these QI results are valuable can be challenging.

Clinicians

Oncologists are usually receptive to using QI methods to help patient selection for clinical trials involving costly targeted therapies and in early identification of responders versus non-responders. Drugs can be stopped in the non-responders, thereby avoiding unnecessary and potentially serious adverse effects and allowing for alternative therapies (110).

Nonetheless, clinicians have reservations regarding the use of QI. Inter- and intraobserver reader variability in QI is well recognized (97, 111). Advances in informatics and computer algorithms will hopefully minimizing this variability. But measurement variance also depends on patients (112, 113). For instance, seemingly minor deviations in patient

preparation such as fasting status may result in considerable variability in SUV measurements. Non-avoidable factors relate to inherent changes in patient physiology that can cause variance in measurement in functional imaging tests (100, 113). Similarly, numerous factors in image generation, such as differences in imaging equipment or the imaging protocol, can cause errors in measured values (114).

Another important pitfall of interpreting QI studies is overconfidence in the results by both the referring clinician and the radiologist (115). Referring clinicians often assume that quantitative results are accurate. They base their clinical decisions on numbers which may be inaccurate for any number of reasons, including: The test was performed incorrectly; the lesion is so small that the numbers provided are inaccurate; there is high inter-radiologist variation. Any of these sources of error lead to inappropriate therapy. For these reasons, a proper quality assurance program addressing acquisition protocols, consistent use of quantitative analysis tools, and standardized reporting methods, is an important part of any department that plans on incorporating QI into its clinical practice.

Manufacturers

To keep pace with rapid advances in molecular medicine, novel QI methods must be developed and validated by manufactures. Significant costs and time are needed for developing new technologies. In many cases, large clinical trials or retrospective analysis of clinical data are needed to show an acceptable level of accuracy, precision, and validity of a given QI method. For some manufacturers, various hurdles for obtaining regulatory clearance act as deterrents in development of novel QI tools (46, 116, 117).

CONCLUSION

Understanding which imaging modalities, organ systems, and disease processes are best served by quantitative imaging will help radiologists accept QI in everyday practice and referring clinicians to use QI to improve and standardize patient care. The adage, “any radiologist with a ruler is dangerous,” has been a part of our specialty's folklore for too long. The time has come to rewrite that folklore. In the new tale, Dan Sullivan's (46) aphorism, “as quantitative as reasonably achievable” will pave the way for improved radiology interpretation and reporting. We hope that radiologists will ultimately embrace the value of QI and incorporate quantitative results into their reports, energized by the tangible benefits to their patients, their referring clinicians, and their own practice.

Acknowledgments

Funding acknowledgements: P30 CA068485 (RGA), P50 CA098131 (RGA), NCI U01CA142565 (TEY), RSNA ESCH1319 (RMS), AHRQ HHSA290201200007I (RMS), T32 EB001631 (JPY)

Dr. Bartholmai is the Principal Investigator for the Radiology Core Laboratory for the NIH/NHLBI-funded Lung Tissue Research Consortium. Mayo has licensed the CALIPER technology shown in the IMBIO, LLC Lung Texture Report and, therefore, Mayo Clinic and Dr. Bartholmai have a financial interest related to this technology.

References

1. Radiological Society of North America. [Accessed on January 12, 2014] Quantitative Imaging Biomarkers Alliance. Available at: http://www.rsna.org/QIBA.aspx

2. Taylor KJ, Burns PN. Duplex Doppler scanning in the pelvis and abdomen. Ultrasound Med Biol. 1985; 11(4):643–58. [PubMed: 2931885]

3. Pearce WH, Astleford P. What's new in vascular ultrasound. Surg Clin North Am. 2004; 84(4): 1113–26. vii. [PubMed: 15261755]

4. Ardalan MR, Tarzamani MK, Shoja MM. A correlation between direct and indirect Doppler ultrasonographic measures in transplant renal artery stenosis. Transplant Proc. 2007; 39(5):1436–8. [PubMed: 17580156]

5. Kruskal JB, Newman PA, Sammons LG, Kane RA. Optimizing Doppler and color flow US: application to hepatic sonography. Radiographics. 2004; 24(3):657–75. [PubMed: 15143220]

6. Kurland BF, Gerstner ER, Mountz JM, Schwartz LH, Ryan CW, Graham MM, et al. Promise and pitfalls of quantitative imaging in oncology clinical trials. Magn Reson Imaging. 2012; 30(9):1301–12. [PubMed: 22898682]

7. Davenport MS, Neville AM, Ellis JH, Cohan RH, Chaudhry HS, Leder RA. Diagnosis of renal angiomyolipoma with hounsfield unit thresholds: effect of size of region of interest and nephrographic phase imaging. Radiology. 2011; 260(1):158–65. [PubMed: 21555349]

8. BLINDED

9. Coursey CA, Nelson RC, Boll DT, Paulson EK, Ho LM, Neville AM, et al. Dual-energy multidetector CT: how does it work, what can it tell us, and when can we use it in abdominopelvic imaging? Radiographics. 2010; 30(4):1037–55. [PubMed: 20631367]

10. Boll DT, Patil NA, Paulson EK, Merkle EM, Simmons WN, Pierre SA, et al. Renal stone assessment with dual-energy multidetector CT and advanced postprocessing techniques: improved characterization of renal stone composition--pilot study. Radiology. 2009; 250(3):813–20. [PubMed: 19244048]

11. Chandarana H, Lim RP, Jensen JH, Hajdu CH, Losada M, Babb JS, et al. Hepatic iron deposition in patients with liver disease: preliminary experience with breath-hold multiecho T2*-weighted sequence. AJR Am J Roentgenol. 2009; 193(5):1261–7. [PubMed: 19843739]

12. Koh DM, Collins DJ. Diffusion-weighted MRI in the body: applications and challenges in oncology. AJR Am J Roentgenol. 2007; 188(6):1622–35. [PubMed: 17515386]

13. Vargas HA, Akin O, Franiel T, Mazaheri Y, Zheng J, Moskowitz C, et al. Diffusion-weighted endorectal MR imaging at 3 T for prostate cancer: tumor detection and assessment of aggressiveness. Radiology. 2011; 259(3):775–84. [PubMed: 21436085]

14. Dimou S, Battisti RA, Hermens DF, Lagopoulos J. A systematic review of functional magnetic resonance imaging and diffusion tensor imaging modalities used in presurgical planning of brain tumour resection. Neurosurgical review. 2013; 36(2):205–14. discussion 14. [PubMed: 23187966]

15. Currie S, Hadjivassiliou M, Craven IJ, Wilkinson ID, Griffiths PD, Hoggard N. Magnetic resonance spectroscopy of the brain. Postgraduate medical journal. 2013; 89(1048):94–106. [PubMed: 23014671]

16. Sakuma H, Takeda K, Higgins CB. Fast magnetic resonance imaging of the heart. Eur J Radiol. 1999; 29(2):101–13. [PubMed: 10374659]

17. Egbert ND, Caoili EM, Cohan RH, Davenport MS, Francis IR, Kunju LP, et al. Differentiation of papillary renal cell carcinoma subtypes on CT and MRI. AJR Am J Roentgenol. 2013; 201(2): 347–55. [PubMed: 23883215]

18. Ho VB, Allen SF, Hood MN, Choyke PL. Renal masses: quantitative assessment of enhancement with dynamic MR imaging. Radiology. 2002; 224(3):695–700. [PubMed: 12202701]

19. Morkenborg J, Pedersen M, Jensen FT, Stodkilde-Jorgensen H, Djurhuus JC, Frokiaer J. Quantitative assessment of Gd-DTPA contrast agent from signal enhancement: an in-vitro study. Magn Reson Imaging. 2003; 21(6):637–43. [PubMed: 12915195]

20. Kuhl CK, Mielcareck P, Klaschik S, Leutner C, Wardelmann E, Gieseke J, et al. Dynamic breast MR imaging: are signal intensity time course data useful for differential diagnosis of enhancing lesions? Radiology. 1999; 211(1):101–10. [PubMed: 10189459]

21. Larsson C, Kleppesto M, Rasmussen I Jr. Salo R, Vardal J, Brandal P, et al. Sampling requirements in DCE-MRI based analysis of high grade gliomas: simulations and clinical results. J Magn Reson Imaging. 2013; 37(4):818–29. [PubMed: 23086710]

22. Hoh CK. Clinical use of FDG PET. Nucl Med Biol. 2007; 34(7):737–42. [PubMed: 17921026]

23. Graham MM, Peterson LM, Hayward RM. Comparison of simplified quantitative analyses of FDG uptake. Nucl Med Biol. 2000; 27(7):647–55. [PubMed: 11091107]
24. Vriens D, de Geus-Oei LF, van Laarhoven HW, Timmer-Bonte JN, Krabbe PF, Visser EP, et al. Evaluation of different normalization procedures for the calculation of the standardized uptake value in therapy response monitoring studies. Nuclear medicine communications. 2009; 30(7): 550–7. [PubMed: 19424100]
25. Chen K, Chen X. Positron emission tomography imaging of cancer biology: current status and future prospects. Semin Oncol. 2011; 38(1):70–86. [PubMed: 21362517]
26. Vallabhajosula S, Solnes L, Vallabhajosula B. A broad overview of positron emission tomography radiopharmaceuticals and clinical applications: what is new? Semin Nucl Med. 2011; 41(4):246–64. [PubMed: 21624560]
27. Gayed I, Vu T, Iyer R, Johnson M, Macapinlac H, Swanston N, et al. The role of 18F-FDG PET in staging and early prediction of response to therapy of recurrent gastrointestinal stromal tumors. J Nucl Med. 2004; 45(1):17–21. [PubMed: 14734662]
28. BLINDED
29. Buckler AJ, Mozley PD, Schwartz L, Petrick N, McNitt-Gray M, Fenimore C, et al. Volumetric CT in lung cancer: an example for the qualification of imaging as a biomarker. Acad Radiol. 2010; 17(1):107–15. [PubMed: 19969254]
30. Kumar V, Gu Y, Basu S, Berglund A, Eschrich SA, Schabath MB, et al. Radiomics: the process and the challenges. Magn Reson Imaging. 2012; 30(9):1234–48. [PubMed: 22898692]
31. McCollough CH, Bruesewitz MR, McNitt-Gray MF, Bush K, Ruckdeschel T, Payne JT, et al. The phantom portion of the American College of Radiology (ACR) computed tomography (CT) accreditation program: practical tips, artifact examples, and pitfalls to avoid. Medical physics. 2004; 31(9):2423–42. [PubMed: 15487722]
32. CT Volumetry Technical Committee. CT Tumor Volume Change Profile, Quantitative Imaging Biomarkers Alliance. Version 2.2. QIBA; Aug 8. 2012 Reviewed DraftAvailable from: http://rsna.org/QIBA_.aspx [Accessed on February 11, 2014]
33. DCE MRI Technical Committee. DCE MRI Quantification Profile, Quantitative Imaging Biomarkers Alliance. Version 1.0. QIBA; Jul 1. 2012 Reviewed DraftAvailable from: http://rsna.org/QIBA_.aspx [Accessed on February 11, 2014]
34. de Langen AJ, Vincent A, Velasquez LM, van Tinteren H, Boellaard R, Shankar LK, et al. Repeatability of 18F-FDG uptake measurements in tumors: a metaanalysis. J Nucl Med. 2012; 53(5):701–8. [PubMed: 22496583]
35. Rockall AG, Avril N, Lam R, Iannone R, Mozley PD, Parkinson C, et al. Repeatability of Quantitative FDG-PET/CT and Contrast-Enhanced CT in Recurrent Ovarian Carcinoma: Test-Retest Measurements for Tumor FDG Uptake, Diameter, and Volume. Clinical cancer research : an official journal of the American Association for Cancer Research. 2014
36. Dachman AH, MacEneaney PM, Adedipe A, Carlin M, Schumm LP. Tumor size on computed tomography scans: is one measurement enough? Cancer. 2001; 91(3):555–60. [PubMed: 11169938]
37. Beer AJ, Wieder HA, Lordick F, Ott K, Fischer M, Becker K, et al. Adenocarcinomas of esophagogastric junction: multi-detector row CT to evaluate early response to neoadjuvant chemotherapy. Radiology. 2006; 239(2):472–80. [PubMed: 16543584]
38. Sosna J, Rofsky NM, Gaston SM, DeWolf WC, Lenkinski RE. Determinations of prostate volume at 3-Tesla using an external phased array coil: comparison to pathologic specimens. Acad Radiol. 2003; 10(8):846–53. [PubMed: 12945918]
39. Zhang J, Kang SK, Wang L, Touijer A, Hricak H. Distribution of renal tumor growth rates determined by using serial volumetric CT measurements. Radiology. 2009; 250(1):137–44. [PubMed: 19092093]
40. Breiman RS, Beck JW, Korobkin M, Glenny R, Akwari OE, Heaston DK, et al. Volume determinations using computed tomography. AJR Am J Roentgenol. 1982; 138(2):329–33. [PubMed: 6976739]

41. Zhao YR, Ooijen PM, Dorrius MD, Heuvelmans M, Bock GH, Vliegenthart R, et al. Comparison of three software systems for semi-automatic volumetry of pulmonary nodules on baseline and follow-up CT examinations. Acta Radiol. 2013
42. Sridhar P, Mercier G, Tan J, Truong MT, Daly B, Subramaniam RM. FDG PET Metabolic Tumor Volume Segmentation and Pathologic Volume of Primary Human Solid Tumors. AJR Am J Roentgenol. 2014; 202(5):1114–9. [PubMed: 24758668]
43. Higano S, Yun X, Kumabe T, Watanabe M, Mugikura S, Umetsu A, et al. Malignant astrocytic tumors: clinical importance of apparent diffusion coefficient in prediction of grade and prognosis. Radiology. 2006; 241(3):839–46. [PubMed: 17032910]
44. Ohba Y, Nomori H, Shibata H, Kobayashi H, Mori T, Shiraishi S, et al. Evaluation of semiquantitative assessments of fluorodeoxyglucose uptake on positron emission tomography scans for the diagnosis of pulmonary malignancies 1 to 3 cm in size. Ann Thorac Surg. 2009; 87(3):886–91. [PubMed: 19231413]
45. van Velzen JE, de Graaf FR, Jukema JW, de Grooth GJ, Pundziute G, Kroft LJ, et al. Comparison of the relation between the calcium score and plaque characteristics in patients with acute coronary syndrome versus patients with stable coronary artery disease, assessed by computed tomography angiography and virtual histology intravascular ultrasound. The American journal of cardiology. 2011; 108(5):658–64. [PubMed: 21684509]
46. Sullivan DC. Imaging as a quantitative science. Radiology. 2008; 248(2):328–32. [PubMed: 18641239]
47. Obenauer S, Hermann KP, Grabbe E. Applications and literature review of the BI-RADS classification. Eur Radiol. 2005; 15(5):1027–36. [PubMed: 15856253]
48. Park JW, Kerbel RS, Kelloff GJ, Barrett JC, Chabner BA, Parkinson DR, et al. Rationale for biomarkers and surrogate end points in mechanism-driven oncology drug development. Clinical cancer research : an official journal of the American Association for Cancer Research. 2004; 10(11):3885–96. [PubMed: 15173098]
49. Pien HH, Fischman AJ, Thrall JH, Sorensen AG. Using imaging biomarkers to accelerate drug development and clinical trials. Drug discovery today. 2005; 10(4):259–66. [PubMed: 15708744]
50. Jaffe TA, Wickersham NW, Sullivan DC. Quantitative imaging in oncology patients: Part 1, radiology practice patterns at major U.S. cancer centers. AJR Am J Roentgenol. 2010; 195(1): 101–6. [PubMed: 20566802]
51. Nishino M, Jagannathan JP, Ramaiya NH, Van den Abbeele AD. Revised RECIST guideline version 1.1: What oncologists want to know and what radiologists need to know. AJR Am J Roentgenol. 2010; 195(2):281–9. [PubMed: 20651182]
52. Benjamin RS, Choi H, Macapinlac HA, Burgess MA, Patel SR, Chen LL, et al. We should desist using RECIST, at least in GIST. J Clin Oncol. 2007; 25(13):1760–4. [PubMed: 17470866]
53. van der Veldt AA, Meijerink MR, van den Eertwegh AJ, Haanen JB, Boven E. Choi response criteria for early prediction of clinical outcome in patients with metastatic renal cell cancer treated with sunitinib. British journal of cancer. 2010; 102(5):803–9. [PubMed: 20145618]
54. Skougaard K, Nielsen D, Jensen BV, Hendel HW. Comparison of EORTC criteria and PERCIST for PET/CT response evaluation of patients with metastatic colorectal cancer treated with irinotecan and cetuximab. J Nucl Med. 2013; 54(7):1026–31. [PubMed: 23572497]
55. National Comprehensive Cancer Network. [Accessed May 5, 2014] Hodgkin Lymphoma. Version 22014. http://www.nccn.org/professionals/physician_gls/pdf/hodgkins.pdf
56. Hamrahian AH, Ioachimescu AG, Remer EM, Motta-Ramirez G, Bogabathina H, Levin HS, et al. Clinical utility of noncontrast computed tomography attenuation value (hounsfield units) to differentiate adrenal adenomas/hyperplasias from nonadenomas: Cleveland Clinic experience. The Journal of clinical endocrinology and metabolism. 2005; 90(2):871–7. [PubMed: 15572420]
57. Koo HJ, Choi HJ, Kim HJ, Kim SO, Cho KS. The value of 15-minute delayed contrast-enhanced CT to differentiate hyperattenuating adrenal masses compared with chemical shift MR imaging. Eur Radiol. 2014
58. Blake MA, Kalra MK, Sweeney AT, Lucey BC, Maher MM, Sahani DV, et al. Distinguishing benign from malignant adrenal masses: multi-detector row CT protocol with 10-minute delay. Radiology. 2006; 238(2):578–85. [PubMed: 16371582]

59. Boland GW, Blake MA, Holalkere NS, Hahn PF. PET/CT for the characterization of adrenal masses in patients with cancer: qualitative versus quantitative accuracy in 150 consecutive patients. AJR Am J Roentgenol. 2009; 192(4):956–62. [PubMed: 19304700]
60. Linton KM, Taylor MB, Radford JA. Response evaluation in gastrointestinal stromal tumours treated with imatinib: misdiagnosis of disease progression on CT due to cystic change in liver metastases. The British journal of radiology. 2006; 79(944):e40–4. [PubMed: 16861316]
61. Bruix J, Sherman M, Llovet JM, Beaugrand M, Lencioni R, Burroughs AK, et al. Clinical management of hepatocellular carcinoma. Conclusions of the Barcelona-2000 EASL conference. European Association for the Study of the Liver. Journal of hepatology. 2001; 35(3):421–30. [PubMed: 11592607]
62. Forner A, Ayuso C, Varela M, Rimola J, Hessheimer AJ, de Lope CR, et al. Evaluation of tumor response after locoregional therapies in hepatocellular carcinoma: are response evaluation criteria in solid tumors reliable? Cancer. 2009; 115(3):616–23. [PubMed: 19117042]
63. Kyriazi S, Collins DJ, Messiou C, Pennert K, Davidson RL, Giles SL, et al. Metastatic ovarian and primary peritoneal cancer: assessing chemotherapy response with diffusion-weighted MR imaging--value of histogram analysis of apparent diffusion coefficients. Radiology. 2011; 261(1): 182–92. [PubMed: 21828186]
64. Srinivasan A, Goyal M, Al Azri F, Lum C. State-of-the-art imaging of acute stroke. Radiographics. 2006; 26(Suppl 1):S75–95. [PubMed: 17050521]
65. Wintermark M, Reichhart M, Thiran JP, Maeder P, Chalaron M, Schnyder P, et al. Prognostic accuracy of cerebral blood flow measurement by perfusion computed tomography, at the time of emergency room admission, in acute stroke patients. Annals of neurology. 2002; 51(4):417–32. [PubMed: 11921048]
66. Lui YW, Tang ER, Allmendinger AM, Spektor V. Evaluation of CT perfusion in the setting of cerebral ischemia: patterns and pitfalls. AJNR American journal of neuroradiology. 2010; 31(9): 1552–63. [PubMed: 20190208]
67. Ma H, Parsons MW, Christensen S, Campbell BC, Churilov L, Connelly A, et al. A multicentre, randomized, double-blinded, placebo-controlled Phase III study to investigate EXtending the time for Thrombolysis in Emergency Neurological Deficits (EXTEND). International journal of stroke : official journal of the International Stroke Society. 2012; 7(1):74–80. [PubMed: 22188854]
68. Parsons MW. Perfusion CT: is it clinically useful? International journal of stroke : official journal of the International Stroke Society. 2008; 3(1):41–50. [PubMed: 18705914]
69. Rai AT, Carpenter JS, Peykanu JA, Popovich T, Hobbs GR, Riggs JE. The role of CT perfusion imaging in acute stroke diagnosis: a large single-center experience. The Journal of emergency medicine. 2008; 35(3):287–92. [PubMed: 18325710]
70. Srinivasan A, Goyal M, Lum C, Nguyen T, Miller W. Processing and interpretation times of CT angiogram and CT perfusion in stroke. The Canadian journal of neurological sciences Le journal canadien des sciences neurologiques. 2005; 32(4):483–6. [PubMed: 16408579]
71. Ogawa T, Shishido F, Kanno I, Inugami A, Fujita H, Murakami M, et al. Cerebral glioma: evaluation with methionine PET. Radiology. 1993; 186(1):45–53. [PubMed: 8380108]
72. Patronas NJ, Di Chiro G, Kufta C, Bairamian D, Kornblith PL, Simon R, et al. Prediction of survival in glioma patients by means of positron emission tomography. Journal of neurosurgery. 1985; 62(6):816–22. [PubMed: 2987440]
73. De Witte O, Lefranc F, Levivier M, Salmon I, Brotchi J, Goldman S. FDG-PET as a prognostic factor in high-grade astrocytoma. Journal of neuro-oncology. 2000; 49(2):157–63. [PubMed: 11206011]
74. Jain R, Ellika SK, Scarpace L, Schultz LR, Rock JP, Gutierrez J, et al. Quantitative estimation of permeability surface-area product in astroglial brain tumors using perfusion CT and correlation with histopathologic grade. AJNR American journal of neuroradiology. 2008; 29(4):694–700. [PubMed: 18202239]
75. Vlieger EJ, Majoie CB, Leenstra S, Den Heeten GJ. Functional magnetic resonance imaging for neurosurgical planning in neurooncology. Eur Radiol. 2004; 14(7):1143–53. [PubMed: 15148622]

76. Wilkinson ID, Romanowski CA, Jellinek DA, Morris J, Griffiths PD. Motor functional MRI for pre-operative and intraoperative neurosurgical guidance. The British journal of radiology. 2003; 76(902):98–103. [PubMed: 12642277]
77. Mitra D, Basu S. Equilibrium radionuclide angiocardiography: Its usefulness in current practice and potential future applications. World journal of radiology. 2012; 4(10):421–30. [PubMed: 23150766]
78. Lund O, Rasmussen K, Jensen FT, Hansen HH. Left ventricular ejection fraction determined with the nuclear stethoscope, gamma camera and contrast ventriculography. Nuclear medicine communications. 1986; 7(5):337–48. [PubMed: 3737030]
79. Fatima N, Zaman MU, Hashmi A, Kamal S, Hameed A. Assessing adriamycin-induced early cardiotoxicity by estimating left ventricular ejection fraction using technetium-99m multiple-gated acquisition scan and echocardiography. Nuclear medicine communications. 2011; 32(5):381–5. [PubMed: 21346663]
80. Klein GJ, Thirion JP. Cardiovascular imaging to quantify the evolution of cardiac diseases in clinical development. Biomarkers : biochemical indicators of exposure, response, and susceptibility to chemicals. 2005; 10(Suppl 1):S1–9.
81. Patil H, O'Keefe J, Thompson R, Bateman T. Role of CT calcium scoring in screening for coronary artery disease. Missouri medicine. 2012; 109(3):193–4. [PubMed: 22860285]
82. Rengier F, Geisbusch P, Schoenhagen P, Muller-Eschner M, Vosshenrich R, Karmonik C, et al. State-of-the-art aortic imaging: Part II - applications in transcatheter aortic valve replacement and endovascular aortic aneurysm repair. VASA Zeitschrift fur Gefasskrankheiten. 2014; 43(1):6–26. [PubMed: 24429327]
83. Augat P, Eckstein F. Quantitative imaging of musculoskeletal tissue. Annual review of biomedical engineering. 2008; 10:369–90.
84. Eckstein F, Cicuttini F, Raynauld JP, Waterton JC, Peterfy C. Magnetic resonance imaging (MRI) of articular cartilage in knee osteoarthritis (OA): morphological assessment. Osteoarthritis and cartilage / OARS, Osteoarthritis Research Society. 2006; 14(Suppl A):A46–75.
85. Eckstein F, Guermazi A, Roemer FW. Quantitative MR imaging of cartilage and trabecular bone in osteoarthritis. Radiol Clin North Am. 2009; 47(4):655–73. [PubMed: 19631074]
86. Sharma L, Eckstein F, Song J, Guermazi A, Prasad P, Kapoor D, et al. Relationship of meniscal damage, meniscal extrusion, malalignment, and joint laxity to subsequent cartilage loss in osteoarthritic knees. Arthritis and rheumatism. 2008; 58(6):1716–26. [PubMed: 18512777]
87. Eckstein F, Wirth W. Quantitative cartilage imaging in knee osteoarthritis. Arthritis. 2011; 2011:475684. [PubMed: 22046518]
88. Rosen BR, Fleming DM, Kushner DC, Zaner KS, Buxton RB, Bennet WP, et al. Hematologic bone marrow disorders: quantitative chemical shift MR imaging. Radiology. 1988; 169(3):799–804. [PubMed: 3187003]
89. Guckel F, Brix G, Semmler W, Ho AD, Korbling M, Georgi M, et al. Proton chemical shift imaging of bone marrow for monitoring therapy in leukemia. Journal of computer assisted tomography. 1990; 14(6):954–9. [PubMed: 2229574]
90. Gerard EL, Ferry JA, Amrein PC, Harmon DC, McKinstry RC, Hoppel BE, et al. Compositional changes in vertebral bone marrow during treatment for acute leukemia: assessment with quantitative chemical shift imaging. Radiology. 1992; 183(1):39–46. [PubMed: 1549692]
91. Hobbins J. Morphometry of fetal growth. Acta paediatrica. 1997; 423:165–8. discussion 9. [PubMed: 9401565]
92. Warsof SL, Cooper DJ, Little D, Campbell S. Routine ultrasound screening for antenatal detection of intrauterine growth retardation. Obstetrics and gynecology. 1986; 67(1):33–9. [PubMed: 3510015]
93. Perinatology.com.. [Accessed on May 5, 2014] Fetal Biometry Calculator II. Perinatology.com.Perinatology.com.Available at http://www.perinatology.com/calculators/biometry.htm.
94. Chauhan SP, Cole J, Sanderson M, Magann EF, Scardo JA. Suspicion of intrauterine growth restriction: Use of abdominal circumference alone or estimated fetal weight below 10%. The journal of maternal-fetal & neonatal medicine : the official journal of the European Association of

Perinatal Medicine, the Federation of Asia and Oceania Perinatal Societies, the International Society of Perinatal Obstet. 2006; 19(9):557–62.

95. Kundel HL. History of research in medical image perception. J Am Coll Radiol. 2006; 3(6):402–8. [PubMed: 17412094]
96. Tuddenham WJ. Roentgen image percetion--a personal survey of the problem. Radiol Clin North Am. 1969; 7(3):499–501. [PubMed: 5382261]
97. Flaherty KR, Andrei AC, King TE Jr. Raghu G, Colby TV, Wells A, et al. Idiopathic interstitial pneumonia: do community and academic physicians agree on diagnosis? American journal of respiratory and critical care medicine. 2007; 175(10):1054–60. [PubMed: 17255566]
98. Jonisch AI, Rubinowitz AN, Mutalik PG, Israel GM. Can high-attenuation renal cysts be differentiated from renal cell carcinoma at unenhanced CT? Radiology. 2007; 243(2):445–50. [PubMed: 17456870]
99. Jaffe TA, Wickersham NW, Sullivan DC. Quantitative imaging in oncology patients: Part 1, radiology practice patterns at major U.S. cancer centers. AJR Am J Roentgenol. 2010; 195(1): 101–6. [PubMed: 20566802]
100. Muzi M, O'Sullivan F, Mankoff DA, Doot RK, Pierce LA, Kurland BF, et al. Quantitative assessment of dynamic PET imaging data in cancer imaging. Magn Reson Imaging. 2012; 30(9): 1203–15. [PubMed: 22819579]
101. Buckler AJ, Mulshine JL, Gottlieb R, Zhao B, Mozley PD, Schwartz L. The use of volumetric CT as an imaging biomarker in lung cancer. Acad Radiol. 2010; 17(1):100–6. [PubMed: 19969253]
102. Motzer RJ, Hutson TE, Tomczak P, Michaelson MD, Bukowski RM, Oudard S, et al. Overall survival and updated results for sunitinib compared with interferon alfa in patients with metastatic renal cell carcinoma. J Clin Oncol. 2009; 27(22):3584–90. [PubMed: 19487381]
103. Thiam R, Fournier LS, Trinquart L, Medioni J, Chatellier G, Balvay D, et al. Optimizing the size variation threshold for the CT evaluation of response in metastatic renal cell carcinoma treated with sunitinib. Ann Oncol. 2010; 21(5):936–41. [PubMed: 19889607]
104. Nathan PD, Vinayan A, Stott D, Juttla J, Goh V. CT response assessment combining reduction in both size and arterial phase density correlates with time to progression in metastatic renal cancer patients treated with targeted therapies. Cancer Biol Ther. 2010; 9(1):15–9. [PubMed: 20009542]
105. Smith AD, Lieber ML, Shah SN. Assessing tumor response and detecting recurrence in metastatic renal cell carcinoma on targeted therapy: importance of size and attenuation on contrast-enhanced CT. AJR Am J Roentgenol. 2010; 194(1):157–65. [PubMed: 20028918]
106. Smith AD, Shah SN, Rini BI, Lieber ML, Remer EM. Morphology, Attenuation, Size, and Structure (MASS) criteria: assessing response and predicting clinical outcome in metastatic renal cell carcinoma on antiangiogenic targeted therapy. AJR Am J Roentgenol. 2010; 194(6):1470–8. [PubMed: 20489085]
107. BLINDED
108. Coxson HO, Whittall KP, Nakano Y, Rogers RM, Sciurba FC, Keenan RJ, et al. Selection of patients for lung volume reduction surgery using a power law analysis of the computed tomographic scan. Thorax. 2003; 58(6):510–4. [PubMed: 12775863]
109. Cederlund K, Bergstrand L, Hogberg S, Rasmussen E, Svane B, Aspelin P. Visual grading of emphysema severity in candidates for lung volume reduction surgery. Comparison between HRCT, spiral CT and “density-masked” images. Acta Radiol. 2002; 43(1):48–53. [PubMed: 11972462]
110. Jaffe TA, Wickersham NW, Sullivan DC. Quantitative imaging in oncology patients: Part 2, oncologists' opinions and expectations at major U.S. cancer centers. AJR Am J Roentgenol. 2010; 195(1):W19–30. [PubMed: 20566776]
111. Sanelli PC, Nicola G, Johnson R, Tsiouris AJ, Ougorets I, Knight C, et al. Effect of training and experience on qualitative and quantitative CT perfusion data. AJNR American journal of neuroradiology. 2007; 28(3):428–32. [PubMed: 17353307]
112. Doot RK, Thompson T, Greer BE, Allberg KC, Linden HM, Mankoff DA, et al. Early experiences in establishing a regional quantitative imaging network for PET/CT clinical trials. Magn Reson Imaging. 2012; 30(9):1291–300. [PubMed: 22795929]

113. Muzi M, O'Sullivan F, Mankoff DA, Doot RK, Pierce LA, Kurland BF, et al. Quantitative assessment of dynamic PET imaging data in cancer imaging. Magn Reson Imaging. 2012; 30(9): 1203–15. [PubMed: 22819579]

114. Gierada DS, Bierhals AJ, Choong CK, Bartel ST, Ritter JH, Das NA, et al. Effects of CT section thickness and reconstruction kernel on emphysema quantification relationship to the magnitude of the CT emphysema index. Acad Radiol. 2010; 17(2):146–56. [PubMed: 19931472]

115. Jha S. The allure of quantification. Magn Reson Imaging. 2013; 31(6):1035–6. [PubMed: 23290481]

116. Buckler AJ, Bresolin L, Dunnick NR, Sullivan DC. A collaborative enterprise for multi-stakeholder participation in the advancement of quantitative imaging. Radiology. 2011; 258(3): 906–14. [PubMed: 21339352]

117. Buckler AJ, Bresolin L, Dunnick NR, Sullivan DC, Aerts HJ, Bendriem B, et al. Quantitative imaging test approval and biomarker qualification: interrelated but distinct activities. Radiology. 2011; 259(3):875–84. [PubMed: 21325035]

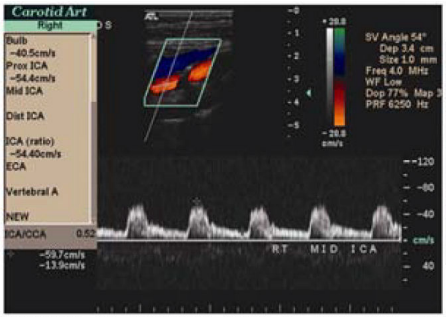

Figure 1.

58-year-old man with concern for carotid artery stenosis. (A) Duplex ultrasound image shows spectral tracing obtained from the mid right internal carotid artery, with measurement of the corresponding peak systolic velocity and end-diastolic velocity. (B) Portion of corresponding radiology report providing findings relating to the right-sided carotid vasculature in tabular format. Based on the provided velocities, it was concluded that the degree of stenosis in the right internal carotid artery is <50%. This lack of hemodynamically significant stenosis, which could not be reliably determined based solely on subjective assessment of the appearance of the vessel, facilitates selection of non-operative management for the patient.

Figure 2.

Volume-rendered image of the hand and wrist from dual-energy CT evaluation in patient with gout, demonstrating use of annotated color-coded volume-rendering to display quantitative results. Pixels with dual-energy absorption characteristics of uric acid crystals are highlighted in green, and the total volume of such pixels is reported. The urate volume can be used as a marker of response to urate-lowering therapy. Parameters used to perform the analysis can be included in the screen capture to facilitate use of similar parameters during follow-up. The image can be captured from the analysis software and stored as a DICOM image as part of the study, along with the original source images.

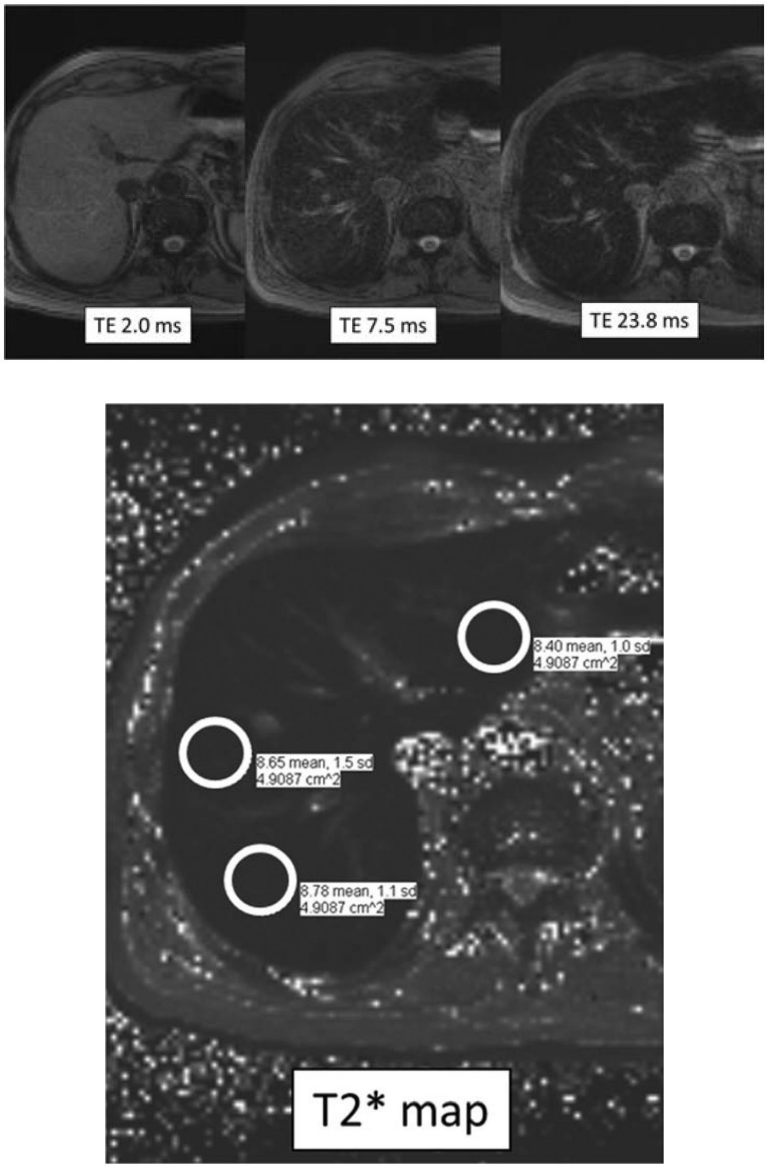

Figure 3.

52-year-old man with a concern for hemochromatosis. (A) Images from a multi-echo T2*-weighted gradient-echo MR acquisition of the liver obtained using echo times (TEs) of 2.0 ms, 7.5 ms, and 23.8 ms. A total of eight different images, with TEs varying between 2.0 ms and 23.8 ms, were obtained. (B) Parametric T2* map was computed from the multi-echo images using a monoexponential fit. T2* values in the liver were in the range of 8–9 ms, consistent with moderate-to-severe hepatic iron deposition. Subjective assessment of multi-echo images indicates the presence of iron, but is limited for determining the severity of iron deposition.

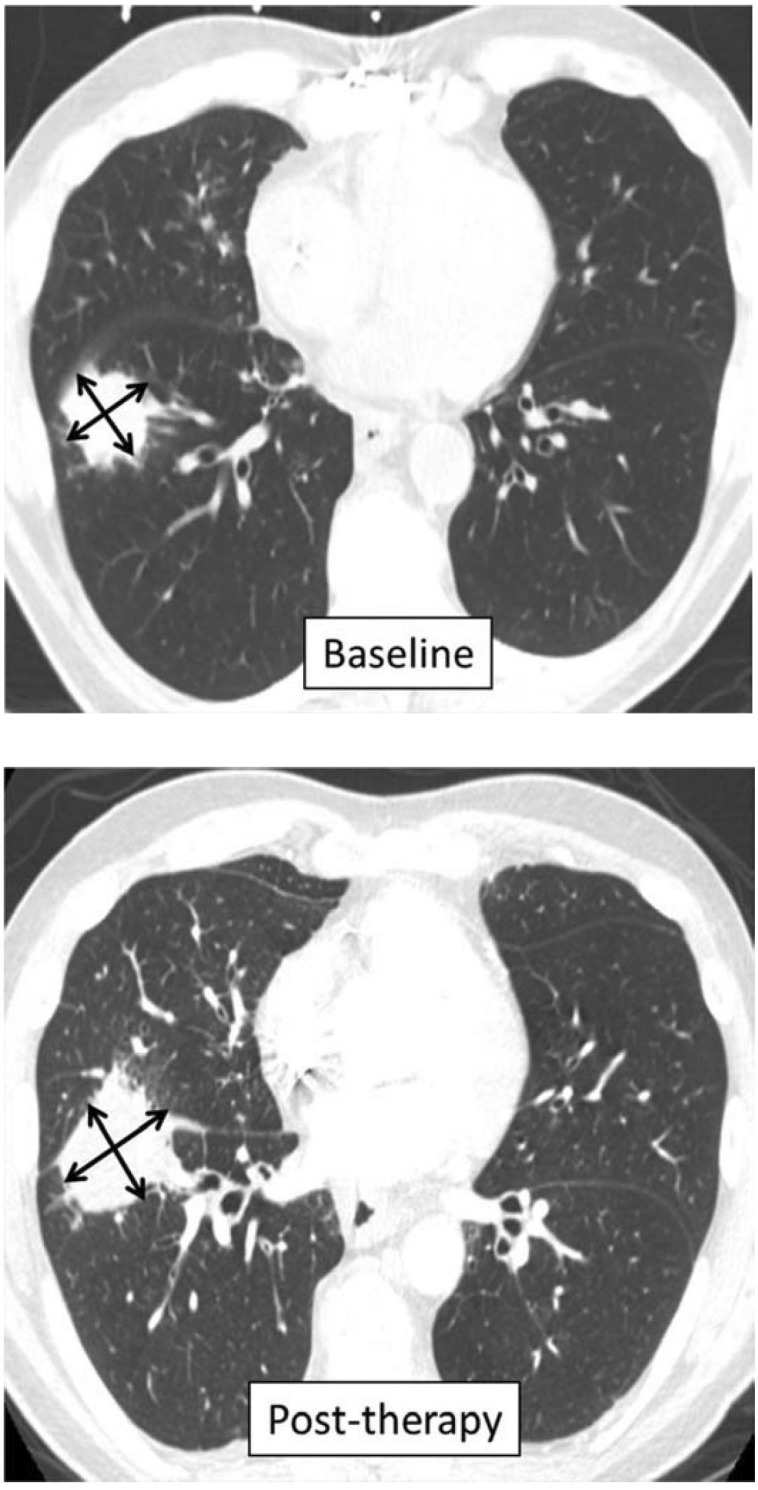

Figure 4.

68-year-old man with lung cancer. (A) Baseline CT image allows determination of lesion volume before treatment (1.5 × 1.7cm). (B) CT image three months later, after

chemotherapy, shows increase in size (2.3 × 2.8cm). These lesion measurements met criteria for progressive disease and resulted in an alteration of the patient's chemotherapy regimen.

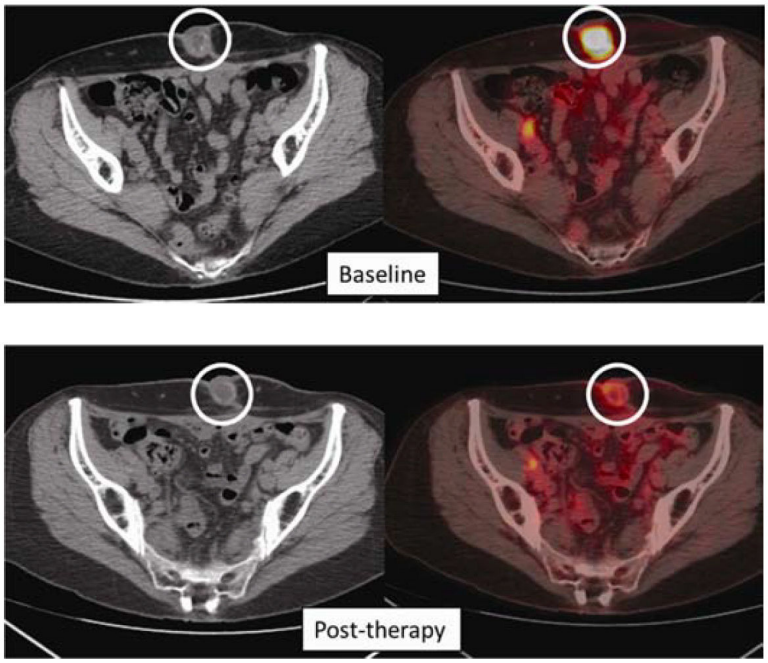

Figure 5.

64-year-old woman with metastatic ovarian cancer. (A) Baseline CT and fused PET/CT images shows an anterior abdominal wall metastasis with marked increased metabolic activity [maximum standardized uptake value (SUVmax) 11.7]. (B) Follow-up CT and fused PET/CT images obtained after 3 months of treatment with paclitaxel shows similar size of the lesion, although there has been substantial interval decrease in metabolic activity (SUVmax 3.7). This interval decrease in SUV is consistent with response to therapy, which is not readily apparent based on evaluation of lesion size alone.

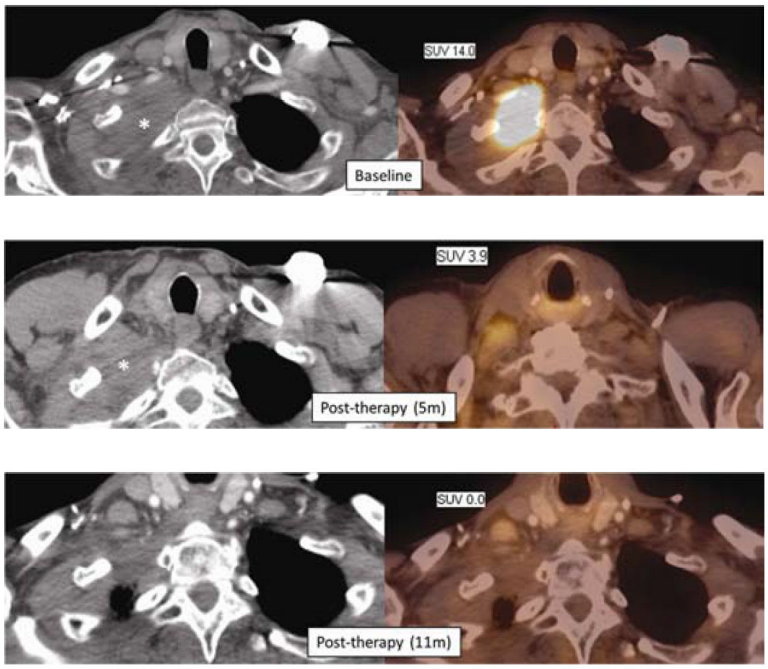

Figure 6.

63-year-old man with Pancoast tumor. (A) Axial CT and fused ^{18}F-FDG PET/CT images demonstrate right apical lung mass with markedly increased metabolic activity; standardized uptake value (SUV) was 14.0 (B) Axial CT and fused PET/CT images obtained five months after radiation and chemotherapy show similar appearance of mass on CT, although SUV has substantially decreased, now measuring 3.9. (C) CT and fused PET/CT images 11 months after treatment shows decreased size of mass on CT, although there is persistent pleural thickening. However, increased metabolic activity has resolved, with SUV now measuring 0.0. The decrease in SUV preceded an appreciable decrease in lesion size.

Figure 7.

62-year-old woman with metastatic breast cancer and a right adrenal nodule. Non-contrast CT image shows the nodule measures -8 Hounsfield units (HU). This measurement meets non-contrast CT criteria for the diagnosis of a benign adrenal adenoma, allowing for the lesion to be characterized as benign. Further evaluation, such as contrast-enhanced CT, MRI, PET, or biopsy, is therefore avoided.

Figure 8.

44-year-old woman undergoing evaluation of left adrenal mass detected on previous imaging. CT using an adrenal washout protocol was performed. Axial CT images show a density of 25 Hounsfield units (HU) in the unenhanced phase (A), not meeting criteria for a lipid-rich adenoma. However, the density was 83 HU in the portal venous phase (B) and 29 HU in the 15-minute delayed phase (C), corresponding with an absolute wash-out ratio (AWR) of 93%. This AWR is greater than a threshold of 60%, indicating with high specificity that the lesion is a benign adenoma.

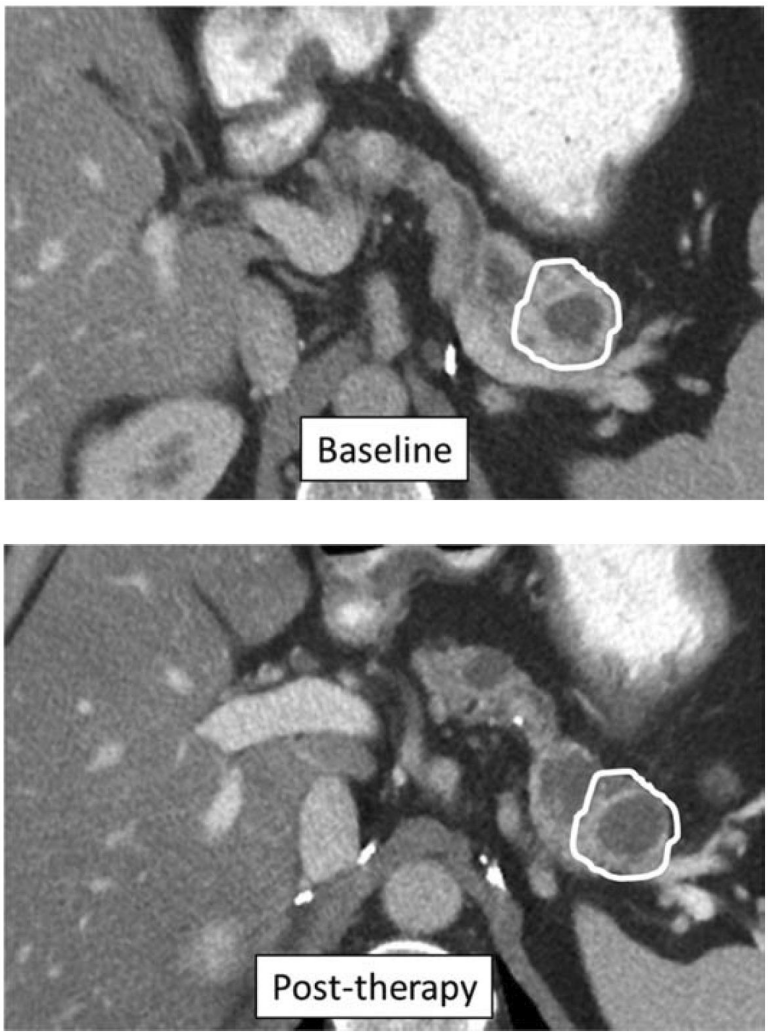

Figure 9.

68-year-old man with metastatic renal cell carcinoma. (A) Baseline CT image shows a cluster of metastatic lesions in the pancreatic tail with decreased attenuation centrally and a hypervascular rim. (B) Follow-up CT image after 3 months of treatment with pazopanib shows similar size of the lesions, although there is decreased attenuation of portions of the lesions compared with the baseline image. This interval decrease in attenuation indicates reduced vascularity due to response to the anti-angiogenic therapy, which is not readily apparent based on evaluation of lesion size alone, and helps guide subsequent treatment decisions.

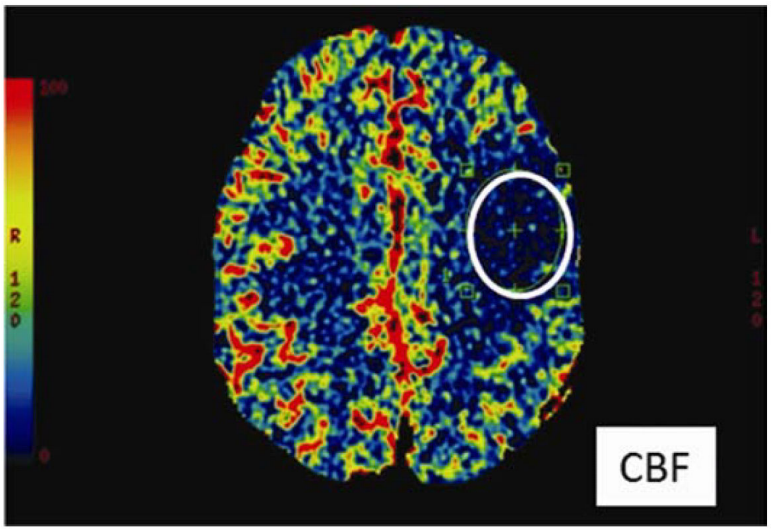

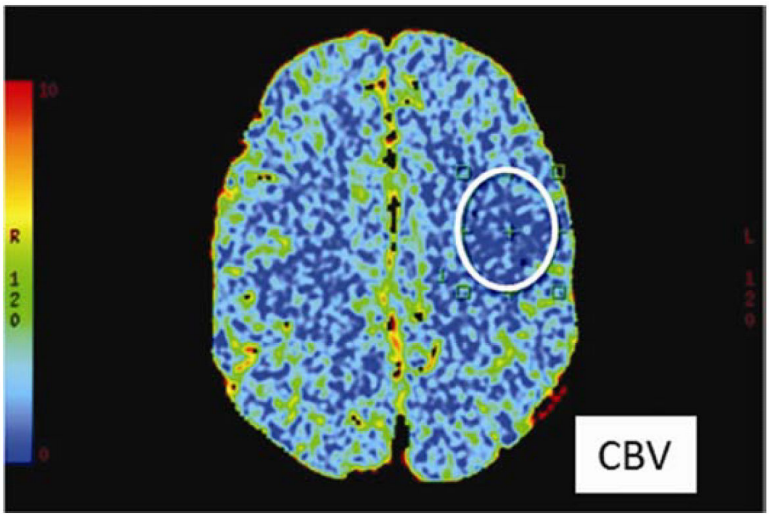

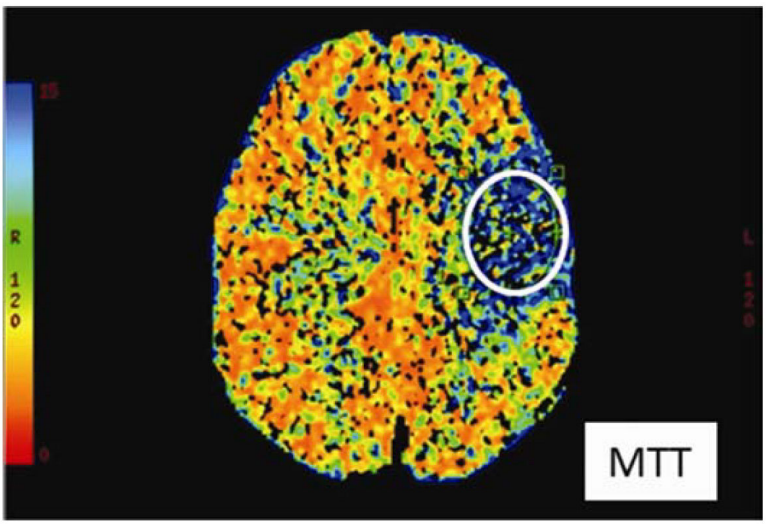

Figure 10.

64-year-old woman with right sided weakness. (A) Parametric map of cerebral blood flow (CBF) shows decreased CBF in the left middle cerebral artery territory. (B) Parametric map of cerebral blood volume (CBV) shows corresponding decreased CBV. (C) Parametric map of mean transit time (MTT) shows corresponding increased MTT. Prolonged MTT over 6 seconds and reduced CBF of 10–15 ml/100g/min are consistent with infarction, indicating permanent damage to this vascular distribution. These measurements contributed to decision to not perform thrombolysis. The assessment of tissue viability was not reliably determined using conventional anatomic imaging alone.

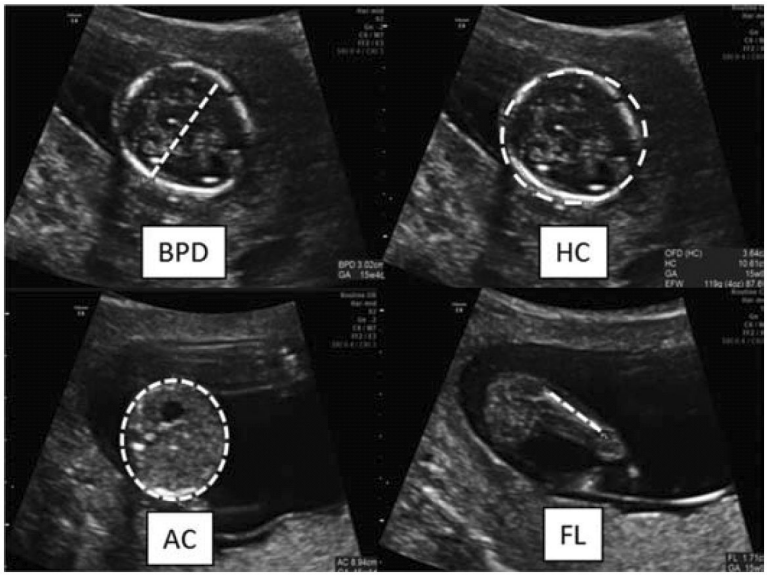

Indication Sonogr.

LMP	01/20/2014	GA(LMP)	14w3d	EDD(LMP)	10/27/2014	G 2	Ab
DOC		GA(AUA)	15w2d	EDD(AUA)	10/21/2014	P 1	Ec

EFW (Hadlock)	Value	Range	Age	Range	GP	Hadlock
AC/BPD/FL/HC	119g (4oz)	± 17g				87.6%

2D Measurements	AUA	Value	m1	m2	m3	Meth.	GP	Age
BPD (Hadlock)	✓	2.98 cm	3.02	2.93		avg.		15w3d
OFD (HC)		3.62 cm	3.64	3.59		avg.		
HC (Hadlock)	✓	10.60 cm	10.61	10.59		avg.		15w0d
AC (Hadlock)	✓	9.05 cm	8.94	9.15		avg.		15w2d
FL (Hadlock)	✓	1.77 cm	1.71	1.82		avg.		15w2d
CRL (Hadlock)	✓	9.59 cm	9.59			avg.	90.5%	15w3d

Doppler Measurements	Value	m1	m2	m3	m4	m5	m6	Meth.
Fetal Heart Rate								
FHR	163 bpm	163						avg.

Figure 11.

23-year-old pregnant woman undergoing fetal survey. (A) Ultrasound biometric measurements include biparietal diameter, head circumference, abdominal circumference, and femur length. (B) Tabular summary uses biometric measurements to provide an estimated fetal gestational age, which can be correlated to gestational age based on last menstrual period, as well as used to compute an estimated fetal weight and growth percentile. These data are used to diagnose fetuses with intrauterine growth restriction.

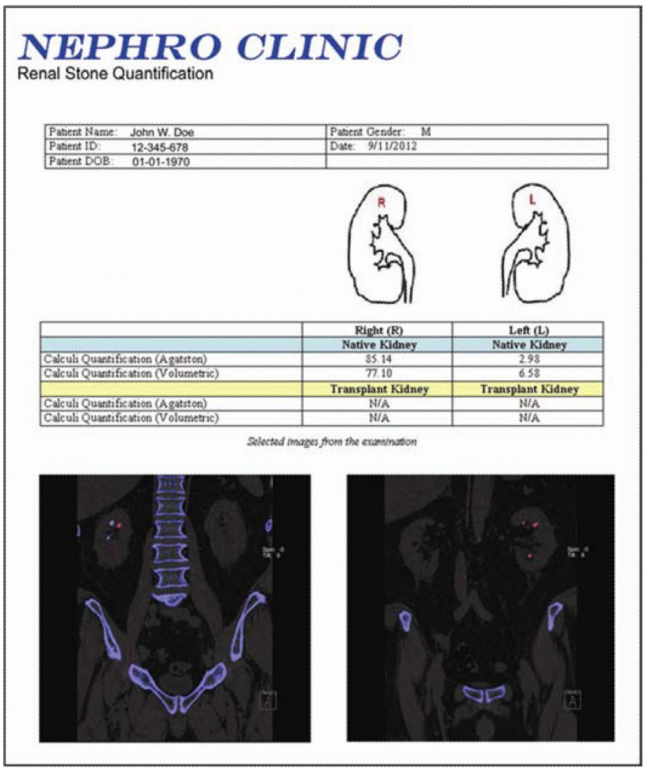

Figure 12.

Sample multimedia report generated for volumetric renal stone quantification assessment in a 40 year-old male with history of nephrolithiasis; report content has been de-identified. This report may be included in the EMR as a scanned document, PDF, screen capture image as part of the DICOM images for the study, or be printed for a paper medical record. The multimedia report generally contains selected images to highlight key findings. A separately generated text report is typically available in the radiology reporting system or associated with the multimedia report as a separate page.

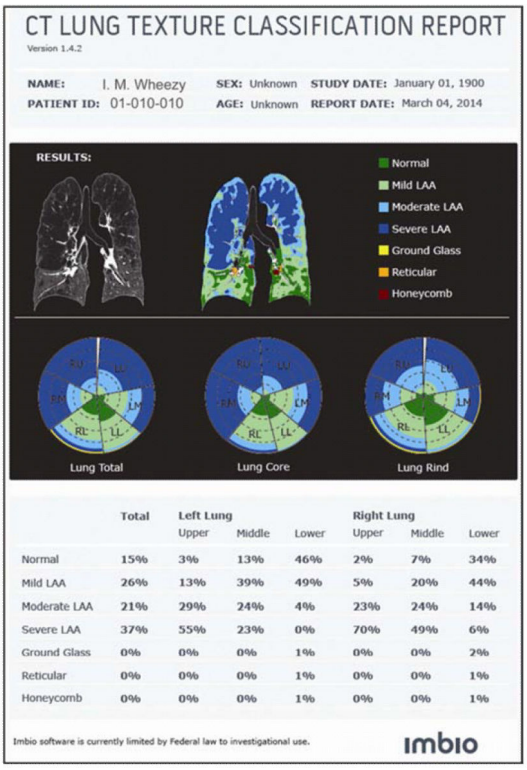

	Total	Left Lung			Right Lung		
		Upper	Middle	Lower	Upper	Middle	Lower
Normal	15%	3%	13%	46%	2%	7%	34%
Mild LAA	26%	13%	39%	49%	5%	20%	44%
Moderate LAA	21%	29%	24%	4%	23%	24%	14%
Severe LAA	37%	55%	23%	0%	70%	49%	6%
Ground Glass	0%	0%	0%	1%	0%	0%	2%
Reticular	0%	0%	0%	1%	0%	0%	1%
Honeycomb	0%	0%	0%	1%	0%	0%	1%

Figure 13.

Sample advanced multimedia report for quantitative lung texture assessment from high-resolution pulmonary CT in 67 year-old male with 110 pack-year smoking history who is a candidate for long volume reduction surgery (LVRS); report content has been de-identified. The pulmonary parenchymal evaluation is performed using CALIPER (Computer-Aided Lung Informatics for Pathology Evaluation and Rating), a CT-based technology developed at Mayo Clinic, that provides qualitative and quantitative assessment of different tissue types for diffuse parenchymal lung diseases based on lung density signatures and morphology. The quantitative analysis shows this patient has upper-lobe predominant disease, and therefore is a potential candidate for LVRS. A segmentation overview, with color overlay of the segmented CT data, is provided in the report. Quantitative results are represented in a summary chart, and colored graphs represent the extent and type of parenchymal classification. (Report courtesy of Imbio, LLC, Minneapolis MN.)

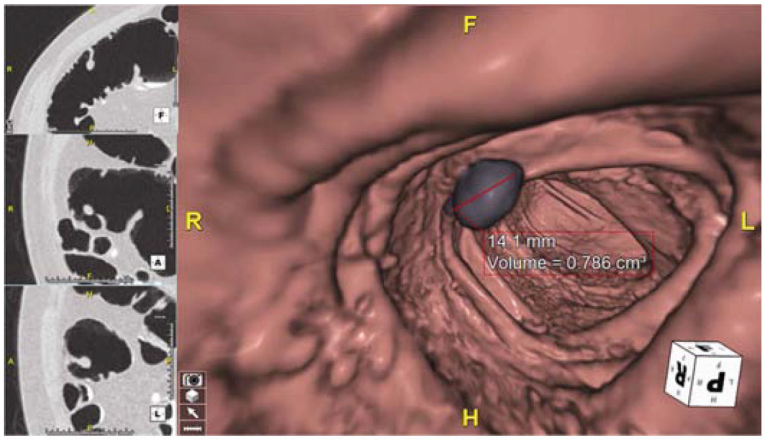

Figure 14.

CT-colonography image in which a pedunculated polyp is colored grey within a surface-shaded rendering of the colon lumen. Polyp diameter and volume are presented as an overlay on the rendering. Case exhibits use of colored and/or annotated renderings to convey quantitative results. The image can be captured from the analysis software and stored as a DICOM image as part of the study, along with the original source images

Table 1

Common Clinical Applications of Quantitative Imaging

	Modality	Measurement	Clinical Application
Tissue Dimensions			
Static:			
	US, CT, MRI	Tumor and nodal dimensions	Tumor staging
	MRI	Articular cartilage thickness, volume and surface area	Osteo arthritis
	US	Fetal dimensions	Fetal health
Dynamic:			
	CT	Tracheal dimensions	Tracheomalacia
	MRI	Cardiac ventricular volumes and ejection fractures	Congestive heart failure, Coronary artery disease, Cardiomyopathy
	Gated nuclear blood pool scintigraphy	Left ventricular volumes and ejection fraction	Congestive heart failure, Coronary artery disease
	Dynamic hepatobiliary scintigraphy	Gallbladder ejection fraction	Chronic cholecystitis
	Gastric emptying scintigraphy	Gastric emptying time	Gastroparesis
Tissue Characterization			
Measurements of pixel values within ROI:	CT	lipid content of adrenal lesions	Differentiation of adenoma and metastasis
	CT	lung attenuation	emphysema
Dynamic time-resolved ROI values:			
	CT	Parenchymal perfusion	Stroke
	DCE MRI	Tumor perfusion	Tumor characterization
Chemical/metabolic:			
	DE CT	Chemical composition	Renal stones
	DE CT	Uric acid crystals	Gout
	CT	Coronary Calcium	Coronary artery disease
	DW MRI	ADC Values	Tumor characterization
	MR	T2* mapping for liver iron	Hemochromatosis
	Chemical shift MRI	Bone marrow composition	Leukemia, lymphoma
	MR	Spectroscopy	Neuro degenerative disorders
	DXA	BMD	Osteoporosis

	Modality	Measurement	Clinical Application
	Renal scintigraphy	Split renal function	Renal insufficiency
	PET	SUV	Tumor characterization
	PET	SUV	Cardiac perfusion
	Thyroid scintigraphy	radioactive iodine uptake	Grave's disease
Vascular Flow	US	Flow velocity	Stenosis
	US	Resistive index and acceleration time	Stenosis
	MRI	Phase-contrast flow quantification	Stenosis
Combinations	CT	RECIST criteria	Tumor response
	CT	Choi criteria	Tumor response